Evidence for three-dimensional *XY* critical properties in underdoped $YBa_2Cu_3O_{7-\delta}$

T. Schneider*
Physik-Institut der Universität Zürich, Winterthurerstrasse 190, CH-8057, Switzerland
(Received 11 October 2006; revised manuscript received 15 April 2007; published 18 May 2007)

We perform a detailed analysis of the reversible magnetization data of Salem-Sugui *et al.* and Babíc *et al.* of underdoped and optimally doped $YBa_2Cu_3O_{7-\delta}$ single crystals. Near the zero field transition temperature we observe extended consistency with the properties of the three-dimensional *XY* universality class, even though the attained critical regime is limited by an inhomogeneity induced finite size effect. Nevertheless, as T_c falls from 93.5 to 41.5 K, the critical amplitude of the in-plane correlation length ξ_{ab0}, the anisotropy $\gamma=\xi_{ab0}/\xi_{c0}$ and the critical amplitude of the in-plane penetration depth λ_{ab0} increase substantially, while the critical amplitude of the *c*-axis correlation length ξ_{c0} does not change much. As a consequence, the correlation volume $V_{\rm corr}^-$ increases and the critical amplitude of the specific heat singularity A^- decreases dramatically, while the rise of λ_{ab0} reflects the behavior of the zero temperature counterpart. Conversely, although ξ_{ab0} and λ_{ab0} increase with reduced T_c, the ratio $\lambda_{ab0}/\xi_{ab0}^-$, corresponding to the Ginzburg-Landau parameter κ_{ab}, decreases substantially and $YBa_2Cu_3O_{7-\delta}$ crosses over from an extreme to a weak type-II superconductor.

DOI: 10.1103/PhysRevB.75.174517 PACS number(s): 74.25.Bt, 74.25.Ha, 74.40.+k

Since the discovery of cuprate superconductors, fluctuation contributions to the specific heat, magnetization, magnetic penetration depths, etc., have been measured in a variety of compounds. In principle, fluctuation studies yield such important information as the universality class onto which these superconductors fall and their effective dimensionality.[1,2] Given the universality class, various properties, e.g., the correlation volume above and below T_c, are no longer independent but related in terms of universal coefficients. As a consequence, the isotope and pressure effects on various properties are no longer independent.[3] In nearly optimally doped $YBa_2Cu_3O_{7-\delta}$, $HgBa_2CuO_{4-\delta}$, and $La_{2-x}Sr_xCuO_4$ the occurrence of three-dimensional (3D)-*XY* criticality is reasonably well established.[4–6] However, in the underdoped regime the anisotropy increases with reduced T_c.[7] Although reduced dimensionality is accompanied with enhanced fluctuations the 3D-*XY* critical regime is expected to shrink. Nevertheless, con-sistency with 3D-*XY* scaling was observed in magnetization measurements of $YBa_2Cu_3O_{7-\delta}$ down to $T_c\simeq 61.4$ K.[5] On the other hand, measurements of the magnetic penetration depth uncovered charged critical behavior in $YBa_2Cu_3O_{6.95}$ sample with $T_c\simeq 61.4$ K.[8] Note that $7-\delta=6.95$ is close to the hole concentration $p\simeq 1/8$ where charge fluctuations are important.[9]

Recently, magnetization measurements have been performed on underdoped $YBa_2Cu_3O_{7-\delta}$ single crystals with $T_c\simeq 41.5$ and 62 K by Salem-Sugui *et al.*[10,11] Here we perform a detailed analysis of these data. In contrast to previous work[4,5] we do not establish the consistency with the 3D-*XY* scaling plots only, but estimate, given the critical exponent of the correlation lengths $\nu\simeq 2/3$, the critical amplitudes of the correlation length, the universal ratios, etc., of the associated fictitious homogeneous system as well. Indeed, the universality class to which a given experimental system belongs is not only characterized by its critical exponents but also by various critical point amplitude ratios and universal coefficients. This is achieved by invoking the limiting behavior of the universal scaling function, allowing to explore the growth of the in-plane and *c*-axis correlation lengths as T_c is approached. The observed limitations of this growth are traced back to a finite size effect, whereupon the correlation lengths cannot grow beyond the extent of the homogenous domains. Clearly, such an analysis does not discriminate between intrinsic or extrinsic inhomogeneities, but it provides lower bounds for the extent of the homogenous domains seen by the relevant fluctuations.

The paper is organized as follows. Next we present a short sketch of the scaling theory and the universal properties appropriate of anisotropic extreme type-II superconductor exhibiting in the absence of an applied magnetic field 3D-*XY* criticality. On this basis we analyze the irreversible magnetization data of Salem-Sugui *et al.*[10,11] and Babíc *et al.*.[5] We observe close to the zero field T_c remarkable consistency with the scaling and critical properties of a finite system belonging to the 3D-*XY* universality class. Indeed, the homogeneity of the samples turns out to be of finite extent, preventing the correlation lengths to grow beyond the extent of the homogeneous regions. Accordingly, the magnetization data does not provide estimates of the scaling and critical properties only, but uncovers the spatial extent of the homogeneous regions as well. As T_c falls from 93.5 to 41.5 K we observe that the critical amplitude of the in-plane correlation length ξ_{ab0}, the anisotropy $\gamma=\xi_{ab0}/\xi_{c0}$, and the critical amplitude of the in-plane penetration depth λ_{ab0} increase substantially, while the critical amplitude of the *c*-axis correlation length does not change much. As a consequence, the correlation volume $V_{\rm corr}^-$ increases and the critical amplitude of the specific heat singularity A^- decreases dramatically, while the rise of λ_{ab0} reflects the behavior of the zero temperature counterpart.[12] Conversely, although ξ_{ab0} and λ_{ab0} increase with reduced T_c, the ratio $\lambda_{ab0}/\xi_{ab0}^-$, corresponding to the Ginzburg-Landau parameter κ_{ab}, decreases substantially and $YBa_2Cu_3O_{7-\delta}$ crosses over from an extreme to a weak type-II superconductor. The rise of the anisotropy with reduced T_c is consistent with a previous magnetic torque study.[13] For the extent of the homogenous domains we derive from the finite size effect in ξ_{ab} and ξ_c the lower bounds $L_{ab}\simeq 367$ Å, $L_c\simeq 53$ Å and $L_{ab}\simeq 254$ Å, $L_c\simeq 53$ Å for the samples of Salem-Sugui *et al.*[10,11] with $T_c\simeq 41.5$ and $T_c\simeq 62$ K, respectively.

To derive the scaling form of the magnetization in the fluctuation dominated regime we note that the scaling of the magnetic field is in terms of the number of flux quanta per correlation area. Thus, when the thermal fluctuations of the order parameter dominate the singular part of the free energy per unit volume of a homogeneous system scales as[1,2,6,14–18]

$$f_s = \frac{Q^{\pm} k_B T}{\xi_{ab}^2 \xi_c} G^{\pm}(z) = \frac{Q^{\pm} k_B T \gamma}{\xi_{ab}^3} G^{\pm}(z), \quad z = \frac{H \xi_{ab}^2}{\Phi_0}. \tag{1}$$

$Q^{\pm}$ is a universal constant and $G^{\pm}(z)$ a universal scaling function of its argument, with $G^{\pm}(z=0)=1$. $\gamma=\xi_{ab}/\xi_c$ denotes the anisotropy, ξ_{ab} the zero-field in-plane correlation length and H the magnetic field applied along the c axis. Approaching T_c the in-plane correlation length diverges as

$$\xi_{ab} = \xi_{ab0}^{\pm} |t|^{-\nu}, \quad t = T/T_c - 1, \quad \pm = \mathrm{sgn}(t). \tag{2}$$

Supposing that 3D-XY fluctuations dominate the critical exponents are given by[19]

$$\nu \simeq 0.671 \simeq 2/3, \quad \alpha = 2\nu - 3 \simeq -0.013, \tag{3}$$

and there are the universal critical amplitude relations[1,2,14–16,19]

$$\frac{\xi_{ab0}^-}{\xi_{ab0}^+} = \frac{\xi_{c0}^-}{\xi_{c0}^+} \simeq 2.21, \quad \frac{Q^-}{Q^+} \simeq 11.5, \quad \frac{A^+}{A^-} = 1.07 \tag{4}$$

and

$$A^- (\xi_{ab0}^-)^2 \xi_{c0}^- = \frac{A^- (\xi_{ab0}^-)^3}{\gamma} = (R^-)^3, \quad R^- \simeq 0.815, \tag{5}$$

where $A^{\pm}$ is the critical amplitude of the specific heat singularity, defined as $c=(A^{\pm}/\alpha)|t|^{-\alpha}+B$. Furthermore, in the 3D-XY universality class T_c, ξ_{c0}^- and the critical amplitude of the in-plane penetration depth λ_{ab0} are not independent but related by the universal relation[1,2,14–16,19]

$$k_B T_c = \frac{\Phi_0^2}{16\pi^3} \frac{\xi_{c0}^-}{\lambda_{ab0}^2} = \frac{\Phi_0^2}{16\pi^3} \frac{\xi_{ab0}^-}{\gamma \lambda_{ab0}^2}. \tag{6}$$

From the singular part of the free energy per unit volume given by Eq. (1) we derive for the magnetization per unit volume $m=M/V=-\partial f_s/\partial H$ the scaling form

$$\frac{m}{TH^{1/2}} = -\frac{Q^{\pm} k_B \gamma}{\Phi_0^{3/2}} F^{\pm}(z), \quad F^{\pm}(z) = z^{-1/2} \frac{dG}{dz}, \tag{7}$$

where

$$z = x^{-1/2\nu} = \frac{(\xi_{ab0}^{\pm})^2 |t|^{-2\nu} H}{\Phi_0}.$$

This scaling form is similar to Prange's[20] result for Gaussian fluctuations. More generally, the existence of the magnetization at T_c, of the penetration depth below T_c and of the magnetic susceptibility above T_c imply the following asymptotic forms of the scaling function,[1,2,6,17,18]

$$Q^{\pm} \left. \frac{1}{\sqrt{z}} \frac{dG^{\pm}}{dz} \right|_{z\to\infty} = Q^{\pm} c_{\infty}^{\pm}, \quad Q^- \left. \frac{dG^-}{dz} \right|_{z\to 0} = Q^- c_0^- (\ln z + c_1),$$

$$Q^+ \left. \frac{1}{z} \frac{dG^+}{dz} \right|_{z\to 0} = Q^+ c_0^+, \tag{8}$$

with the universal coefficients[1,6]

$$Q^- c_0^- \simeq -0.7, \quad Q^+ c_0^+ \simeq 0.9, \quad q = Q^{\pm} c_{\infty}^{\pm} \simeq 0.5. \tag{9}$$

The scaling form (7) with the limits (8), together with the critical exponents [Eq. (3)] and the universal relations (4) and (6) are characteristic properties of the 3D-XY universality class. Accordingly, a homogeneous extreme type-II superconductor falls into this universality class when these relations are satisfied. When this is the case the doping dependence of the nonuniversal critical properties, such as transition temperature T_c, critical amplitudes of correlation lengths $\xi_{ab0,c0}^{\pm}$, anisotropy γ, etc., can be determined, while the universal relations are independent of the doping level.

To determine T_c we consider the limit $z\to\infty$ $(x\to 0)$. Here the scaling form (7) reduces with Eq. (8) to

$$\frac{m}{H^{1/2}} = -\frac{k_B q}{\Phi_0^{3/2}} \gamma T, \quad q = Q^{\pm} c_{\infty}^{\pm}. \tag{10}$$

$Q^+ c_{\infty}^+ = Q^- c_{\infty}^-$ follows from the fact that $m/\sqrt{H_c}$ adopts at the zero-field transition temperature T_c a unique value where the curves $m/\sqrt{H}$ vs T taken at different fields H cross and $m/H^{1/2}\gamma T_c$ adopts the universal value

$$\frac{m}{H^{1/2} T_c \gamma} = -\frac{k_B q}{\Phi_0^{3/2}}. \tag{11}$$

Furthermore, at T_c and in the limit $H\to 0$ Eq. (10) also implies

$$\frac{m}{HT_c} = -\frac{k_B q \gamma}{\Phi_0^{3/2}} \frac{1}{H^{1/2}}, \tag{12}$$

describing the divergence of the diamagnetic susceptibility at T_c when $H\to 0$. Accordingly, the location of a crossing point in $m/\sqrt{H}$ vs T provides an estimate for the 3D transition temperature and the factor of proportionality in $m/(HT_c)$ vs $H^{1/2}$ probes the anisotropy γ.

Given then T_c and with that the reduced temperature $t=T/T_c-1$, the dominant fluctuations and their properties can now be explored by invoking the scaling form (7). Considering the plot $M/(TH^{1/2})$ vs bt for various fixed magnetic fields H, evidence for 3D-XY fluctuations is established when according to Eq. (7) b scales as $b\propto H^{1/2\nu}$ with $\nu \simeq 2/3$. As $YBa_2Cu_3O_{7-\delta}$ near optimum doping is concerned this scaling behavior is well confirmed.[4,5] However, more detailed properties of the 3D-XY universality class, as well as the doping dependence of critical amplitudes, can be derived by invoking the limiting forms (8) of the scaling function. Considering the limit $z\to 0$, Eq. (7) reduces below T_c to

$$\frac{m}{T} = -\frac{Q^- c_0^- k_B}{\Phi_0 \xi_c^-} \left[\ln\left(\frac{H(\xi_{ab})^2}{\Phi_0} \right) + c_1 \right], \tag{13}$$

and above T_c to

$$\frac{m}{TH} = -\frac{Q^+ c_0^+ k_B (\xi_{ab})^2}{\Phi_0^2 \xi_c}. \tag{14}$$

Thus, given the magnetization data of a homogenous system, attaining the limit $z = H(\xi_{ab0}^{\pm})^2 |t|^{-2\nu}/\Phi_0 \ll 1$, the growth of ξ_{ab} and ξ_c is unlimited and estimates for ξ_{c0}^-, ξ_{ab0}^+ and $(\xi_{ab0}^+)^2/\xi_{c0}^+$ can be deduced from

$$|t|^{-2/3}\frac{m}{T} = -\frac{Q^- c_0^- k_B}{\Phi_0 \xi_{c0}^-}\left[\ln\left(\frac{H(\xi_{ab0}^-)^2}{\Phi_0}\right) + \ln|t|^{-4/3} + c_1\right] \tag{15}$$

and

$$|t|^{2/3}\frac{m}{TH} = -\frac{Q^+ c_0^+ k_B (\xi_{ab0}^+)^2}{\Phi_0^2 \xi_{c0}^+}, \tag{16}$$

given the values for the universal constants $Q^- c_0^-$ and $Q^+ c_0^+$ [Eq. (9)]. However, for data taken at fixed magnetic field the reduction of $z = [H(\xi_{ab0}^+)^2/\Phi_0]|t|^{-4/3}$ unavoidably implies an increasing reduced temperature t and with that a run away from criticality. Thus, for fixed magnetic field the window where these limiting forms apply is limited to intermediate values of the reduced temperature.

In spite of intrinsic inhomogeneities and disorder in cuprate superconductors there is considerable evidence for 3D-*XY* critical behavior, except for a rounded transition close to T_c.[1,2,4,5,15–18,21–26] As disorder is concerned there is the Harris criterion,[27] which states that short-range correlated and uncorrelated disorder is irrelevant at the unperturbed critical point, provided that the specific heat exponent α is negative. Since in the 3D-*XY* universality class α is negative [Eq. (3)], disorder is not expected to play an essential role. However, when superconductivity is restricted to homogeneous domains of finite spatial extent $L_{ab,c}$, the system is inhomogeneous and the resulting rounded transition uncovers a finite size effect[28,29] because the correlation lengths $\xi_{ab,c} = \xi_{ab0,c0}^{\pm}|t|^{-\nu}$ cannot grow beyond $L_{ab,c}$, the respective extent of the homogenous domains. Hence, as long as $\xi_{ab,c} < L_{ab,c}$ the critical properties of the fictitious homogeneous system can be explored with the aid of Eqs. (15) and (16). There is considerable evidence that this scenario accounts for the rounded transition seen in the specific heat[1] and the magnetic penetration depths.[30] As the magnetization is concerned the finite size effect is expected to set in close to T_c where $\xi_{ab,c}$ approaches $L_{ab,c}$. When $\xi_c < L_c$ and ξ_{ab} reaches L_{ab} a finite size effect appears in the plot $|t|^{-2/3}m/T$ vs $\ln|t|^{-4/3}$ around $\ln|t_{abp}|^{-4/3}$ ($\xi_{ab0}^-|t_{abp}|^{-4/3} = L_{ab}$) as the onset of deviations from the linear behavior. Even closer to T_c where both ξ_{ab} and ξ_c attain the respective limiting length, (m/T) tends according to Eq. (13) to diverge as $f_0|t|^{-2/3}$, where $f_0 = -(Q^- c_0^- k_B)/(\Phi_0 L_c)[\ln(HL_{ab}^2/\Phi_0) + c_1]$. Accordingly, sufficiently extended magnetization data are not expected to provide estimates for the critical properties of the associated fictitious homogeneous system only, but do have the potential to uncover inhomogeneities giving rise to a finite size effect as well. As a unique size of the homogeneous domains is unlikely, the smallest extent will set the scale where the growth of the respective correlation length starts to deviate from the critical behavior of the homogenous counterpart. Furthermore, when the outlined analysis of magnetization data uncovers 3D-*XY* universality, it also implies that the pressure and isotope effects on the critical properties are not independent but related in terms of universal relations such as Eqs. (4)–(6) and (10). As an example, the universal form (10) implies that the pressure or isotope exchange induced changes of magnetization, transition temperature and anisotropy are related by $\Delta m(T_c)/m(T_c) = \Delta T_c/T_c + \Delta\gamma(T_c)/\gamma(T_c)^3$. Last but not least, it provides estimates for the pressure and isotope effects on the critical amplitudes, the correlation lengths, the transition temperature, the anisotropy and the extent of the homogeneous domains.

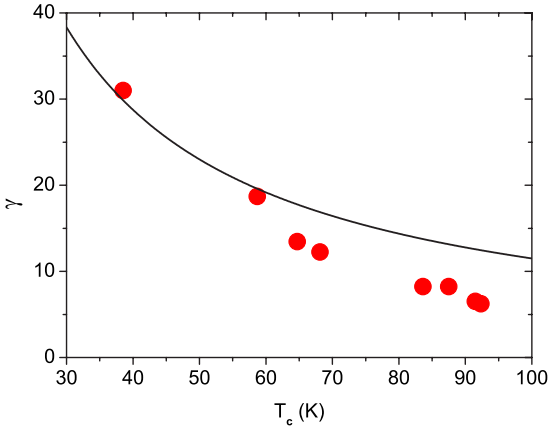

FIG. 1. (Color online) γ vs T_c for $YBa_2Cu_3O_{7-\delta}$ derived from Janossy *et al.* (Ref. 13). To estimate γ for the T_c's considered here we use $\gamma = 1150/T_c$ indicated by the solid line.

We are now prepared to analyze the reversible magnetization data of Salem-Sugui *et al.*[10,11] for underdoped $YBa_2Cu_3O_{7-\delta}$ single crystals with $T_c \simeq 41.5$ K and $T_c \simeq 62$ K. From magnetic torque measurements it is known that in the underdoped regime the chemical substitution tuned reduction of T_c is accompanied by an increase of the anisotropy. From Fig. 1, showing γ vs T_c it is seen that γ increases from 6 around $T_c \simeq 91$ K to 29 near $T_c \simeq 40$ K.

Sufficiently close to T_c 3D-*XY* fluctuations are expected to dominate. In this case Eq. (10) implies the occurrence of a crossing point in $M/H^{1/2}$ vs T at T_c. The plots shown in Fig. 2 uncover these crossing points and provide for the respective transition temperatures the estimates $T_c \simeq 41.5$ and 62 K.

To identify the dominant fluctuations further we plotted the magnetization data of Salem-Sugui *et al.*[10,11] for the underdoped $YBa_2Cu_3O_{7-\delta}$ single crystals with $T_c \simeq 41.5$ K in Fig. 3, in terms of $M/(TH^{1/2})$ vs bt with b adjusted to achieve a collapse on the $H = 0.1$ T curve close to $t = 0$. According to Eq. (7) the dominance of 3D-*XY* fluctuations is established when b scales as $b \propto 1/H^{1/2\nu} \propto 1/H^{3/4}$. In the inset of Fig. 3, showing the field dependence of b, we observe remarkable consistency with the characteristic 3D-*XY* behavior. Near $bt = 0$ the data is seen to collapse within experimental accuracy, while the quality of the collapse deteriorates with increasing field.

According to Fig. 4, showing the corresponding plots for the sample with $T_c \simeq 62$ K, we observe again consistency with the characteristic 3D-*XY* critical behavior $b \simeq H^{-3/4}$.

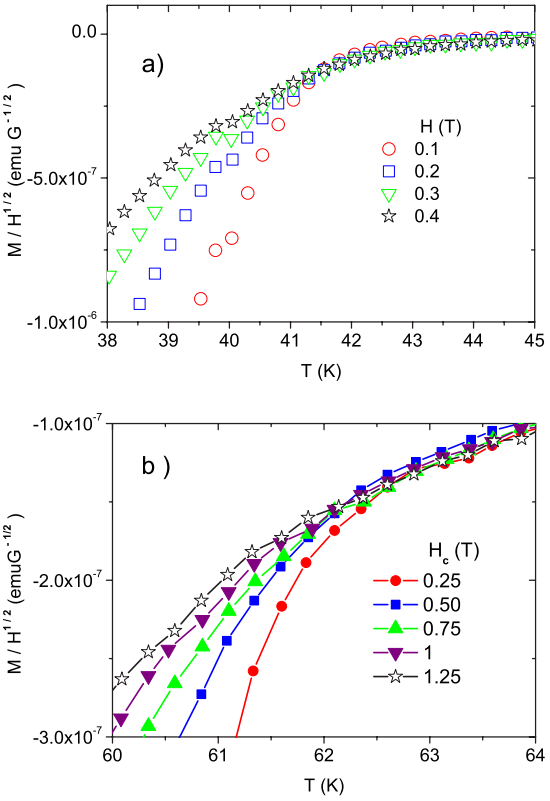

FIG. 2. (Color online) $M/H^{1/2}$ vs T at various fixed magnetic fields H applied along the c axis of underdoped $YBa_2Cu_3O_{7-\delta}$ single crystals with $T_c \simeq 41.5$ K (a) and $T_c \simeq 62$ K (b) derived from the data of Salem-Sugui *et al.* (Refs. 10 and 11). The crossing points provide an estimate for the respective transition temperature, $T_c \simeq 41.5$ K (a) and $T_c \simeq 62$ K (b).

Even though the data collapse is seen to deteriorate with increasing field as well, these plots uncover the dominance of 3D-XY fluctuations around the estimated transition temperature T_c.

A stringent scaling relation to clarify the evidence for 3D-XY critical behavior further, is $M(T_c,H)/(T_cH) \propto H^{-1/2}$, given by Eq. (12). Indeed, it differs substantially from the corresponding 2D-XY behavior, $M(T_c,H)/(T_cH) \propto H^{-1}$ (Ref. 1). In Fig. 5 we depicted $M/(T_cH)$ vs H for the underdoped $YBa_2Cu_3O_{7-\delta}$ single crystals with $T_c \simeq 41.5$ and 62 K, derived from the data of Salem-Sugui *et al.*[10] While the less anisotropic sample with $T_c \simeq 62$ K exhibits remarkable consistency with the 3D-XY behavior over the entire range, indicated by the solid line, the more anisotropic sample with $T_c \simeq 41.5$ K approaches this behavior, indicated by the dashed line, for low fields only. At higher fields a crossover to the 2D-XY behavior $M(T_c,H)/(T_cH) \propto H^{-1}$, indicated by the dotted line, can be anticipated. In the highly anisotropic $Bi_2Sr_2CaCu_2O_{8+\delta}$ with $T_c \simeq 84$ K the analysis of the magnetization data of Li *et al.*[31] uncovers agreement with the 2D behavior $M(T_c,H)/(T_cH) \propto H^{-1}$ from $H=5$ to 10^5 Oe. However, in the limit $H \to 0$ a crossover to 3D behavior is expected to occur because superconductivity is known to be a 3D phenomenon, even in the highly anisotropic $Bi_2Sr_2CaCu_2O_{8+\delta}$. In any case, the stringent scaling plot shown in Fig. 5 reveals that in the underdoped $YBa_2Cu_3O_{7-\delta}$ single crystals considered here 3D-XY critical behavior dominates sufficiently close to T_c. On the contrary, Salem-Sugui *et al.*[32] suggested that the magnetization data of under-

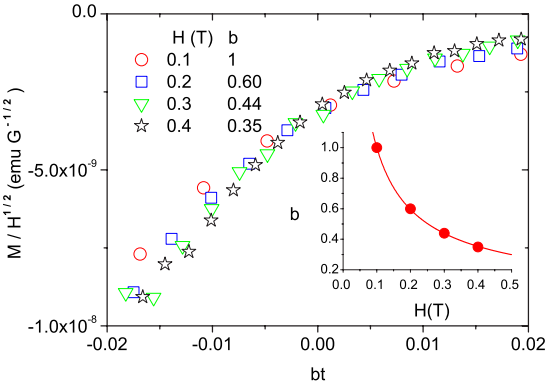

FIG. 3. (Color online) $M/(TH^{1/2})$ vs bt with b adjusted to achieve a collapse on the $H=0.1$ T data of Salem-Sugui *et al.* (Refs. 10 and 11) for the underdoped $YBa_2Cu_3O_{7-\delta}$ single crystals with $T_c \simeq 41.5$ K. The inset shows b vs H. The solid line is $b \propto H^{-3/4}$ characteristic for 3D-XY thermal fluctuations.

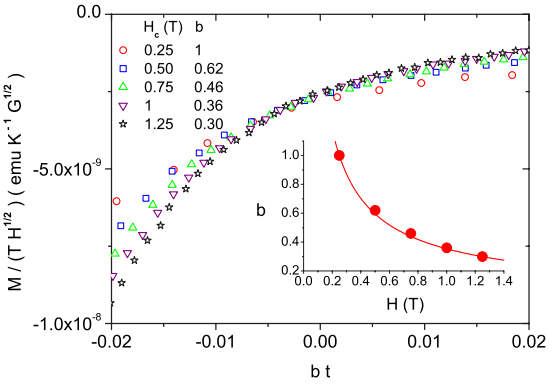

FIG. 4. (Color online) $M/(TH^{1/2})$ vs bt with b adjusted to achieve a collapse on the $H_c=0.25$ T curve for the data shown in Fig. 3(b). The inset shows b vs H. The solid line is $b \propto H^{-3/4}$, characteristic for 3D-XY thermal fluctuations.

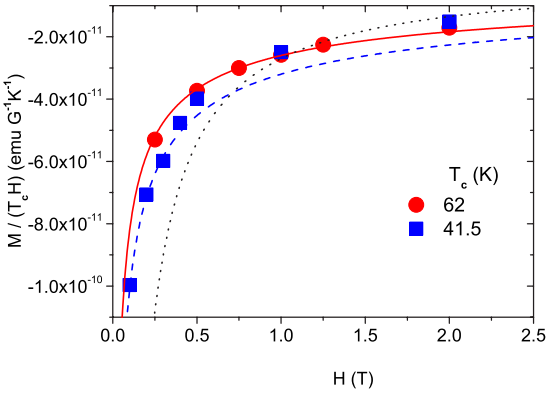

FIG. 5. (Color online) $M/(T_cH)$ vs H of underdoped $YBa_2Cu_3O_{7-\delta}$ single crystals with $T_c \simeq 41.5$ K (■) and $T_c \simeq 62$ K (●) derived from Salem-Sugui *et al.* (Ref. 10). The dashed line is $M/(T_cH) = -3.2 \times 10^{-11}/H^{1/2}$, the solid line $M/(T_cH) = -2.6 \times 10^{-11}/H^{1/2}$, and the dotted one $M/(T_cH) = -2.7 \times 10^{-11}/H$.

TABLE I. T_c, weight of the samples $m=M\rho$/weight with $\rho \simeq 6.3$ g/cm (Ref. 33) and $\widetilde{\Delta T^{\pm}}/T_c$.

T_c (K)	weight (mg)	m (emu cm^{-3})	$\widetilde{\Delta T^{-}}/T_c$	$\widetilde{\Delta T^{+}}/T_c$
441.5	1	6300 M	0.04	0.01
62	1.2	5250 M	0.04	0.01

doped $YBa_2Cu_3O_{7-\delta}$ single crystals with $T_c \simeq 41.5$ K and $T_c \simeq 52$ K point to 2D critical behavior for low magnetic fields and 3D behavior for high fields.[33]

Having established the consistency with 3D-*XY* universality in terms of scaling plots based on the universal scaling forms (7) and (12) with $\nu \simeq 2/3$ and the estimates for T_c we are no prepared to perform a more detailed analysis providing additional checks, allowing to explore the inhomogeneity induced finite size effects and to estimate the essential critical properties, including the critical amplitudes of the correlation lengths and the anisotropy. The basic starting point is either the limiting behavior below or above T_c, given by Eqs. (15) and (16), respectively. To invoke these limiting forms it is necessary to convert the magnetization data M given in emu to m in emu cm^{-3} according to Table I.

Next we invoke the limiting form Eq. (15) to estimate the magnitude of the critical amplitudes below T_c and to explore the homogeneity of the samples. For this purpose we depicted in Fig. 6 $|t|^{-2/3}m/T$ vs $\ln|t|^{-4/3}$. In both samples we observe in a limited interval consistency with the asymptotic behavior, indicated by the straight lines. Using Eqs. (9) and (15) we derive from the slope of these lines the estimates

$$\xi_{c0} \simeq 1.46 \text{ Å } (T_c \simeq 41.5 \text{ K}), \quad \xi_{c0} \simeq 1.33 \text{ Å } (T_c \simeq 62 \text{ K}), \tag{17}$$

for the critical amplitude of the c-axis correlation length.

From the straight lines in Fig. 6 it also follows that

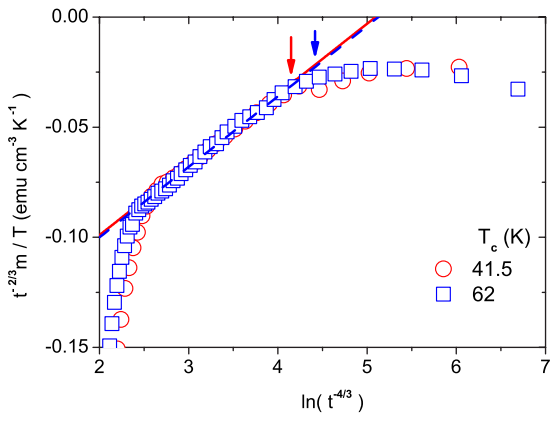

FIG. 6. (Color online) $|t|^{-2/3}m/T$ vs $\ln|t|^{-4/3}$ for $t<0$. (○) sample with $T_c \simeq 41.5$ K at $H=0.1$ T; the solid line is $|t|^{-2/3}m/T = -0.163+0.032\ln|t|^{-4/3}$. The arrow marks $\ln|t_{abp}|^{-4/3} \simeq 4.12$ ($t_{abp} \simeq -0.045$). (□) sample with $T_c \simeq 62$ K at $H=0.5$ T; the dashed line is $|t|^{-2/3}m/T = -0.164+0.032\ln|t|^{-4/3}$. The dashed arrow marks $\ln|t_{abp}|^{-4/3} \simeq 4.23$ ($t_{abp} \simeq -0.042$).

$$\ln \frac{10^3(\xi_{ab0})^2}{\Phi_0} = -5.09 - c_1 \ (T_c \simeq 41.5 \text{ K}),$$

$$\ln \frac{2.5 \times 10^3(\xi_{ab0})^2}{\Phi_0} = -5.39 - c_1 \ (T_c \simeq 62), \tag{18}$$

yielding for the critical amplitudes of the in-plane correlation lengths the ratio

$$\frac{\xi_{ab0}(T_c \simeq 41.5 \text{ K})}{\xi_{ab0}(T_c \simeq 62 \text{ K})} \simeq 1.54. \tag{19}$$

In addition, this plot reveals that the attainable critical regime, indicated by the straight lines, ends around the marked values $\ln|t_{abp}|^{-4/3} \simeq 4.12$ and $\ln|t_{abp}|^{-4/3} \simeq 4.46$. Here the in-plane correlation length ξ_{ab} reaches the limiting length L_{ab}, so that $\xi_{ab0}|t_{abp}|^{-2/3} = L_{ab}$. From $\ln|t_{abp}|^{-4/3} \simeq 4.12$ and $\ln|t_{abp}|^{-4/3} \simeq 4.46$ and Eq. (19) we obtain for the ratio between the limiting lengths L_{ab} the estimate

$$\frac{L_{ab}(T_c \simeq 41.5 \text{ K})}{L_{ab}(T_c \simeq 62 \text{ K})} \simeq 1.36. \tag{20}$$

Nevertheless, given the estimate for the universal coefficient c_1, we can extract from Eq. (18) the critical amplitude of the in-plane correlation length of the respective fictitious homogeneous system. Using $c_1=1.76$, which will be derived later on, we obtain

$$\xi_{ab0} \simeq 46.82 \text{ Å}: \quad T_c \simeq 41.5 \text{ K},$$
$$\xi_{ab0} \simeq 27.32 \text{ Å}: \quad T_c \simeq 62 \text{ K}' \tag{21}$$

and together with the values for ξ_{c0} [Eq. (17)] for the anisotropy

$$\gamma \simeq 32.07: \quad T_c \simeq 41.5 \text{ K},$$
$$\gamma \simeq 20.5: \quad T_c \simeq 62 \text{ K}, \tag{22}$$

in reasonable agreement with the estimates derived from the magnetic torque measurements, namely, $\gamma \simeq 28$ and 19 (see Fig. 1).

Given the critical amplitude of the c-axis correlation length [Eq. (17)] and the interlayer spacing $s \simeq 12$ Å the temperature regime $\Delta T^{\pm} = |T - T_c|$ where 3D behavior occurs is readily estimated from $\Delta T^{\pm} < \Delta\tilde{T}^{\pm} = T_c(\xi_{c0}^{\pm}/s)^{3/2}$. Indeed, the system behaves quasi-2D when ξ_c drops below the interlayer separation s. In Table I we listed the resulting values for $\Delta\tilde{T}^{\pm}/T_c$ which are consistent with the regime where Figs. 3 and 4 reveal a collapse of the data.

To analyze the behavior closer to T_c we consider the plot $-|t|^{-2/3}m/T$ vs $-t$ shown in Fig. 7. Above $t_{abp} \simeq 0.046$ and $t_{abp} \simeq 0.034$ there is an interval exhibiting the $\ln|t|^{-4/3}$ behavior of a homogeneous system, indicated by the solid curve and consistent with the $|t|^{-2/3}m/T$ vs $\ln|t|^{-4/3}$ plots shown in Fig. 6. Indeed, a minimum occurs below t_{abp} followed by an increase. Although the data is sparse, it indicates a $|t|^{-2/3}$ divergence, associated with a finite size effect in both, ξ_{ab} and ξ_c, whereby these correlation lengths cannot grow beyond L_{ab} and L_c, respectively. According to Eq. (15) the amplitude of the divergence is given by

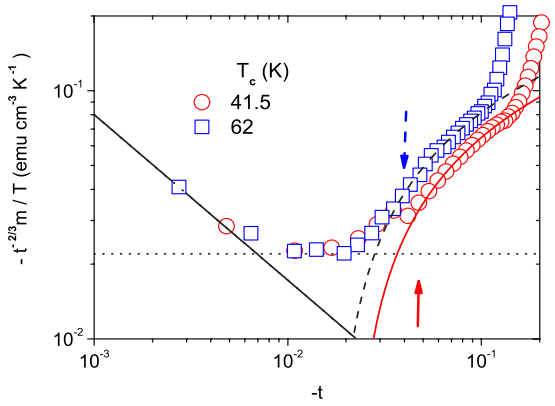

FIG. 7. (Color online) $-|t|^{-2/3}m/T$ vs $-t$ for $t<0$. (○) sample with $T_c \simeq 41.5$ K at $H=0.1$ T; the solid curve is $-|t|^{-2/3}m/T=0.15-0.03\ln|t|^{-4/3}$ and the dashed one $-|t|^{-2/3}m/T=8.10^{-4}|t|^{-2/3}$. The arrow marks $t_{abp}\simeq -0.047$ ($\ln|t_{abp}|^{-4/3}\simeq 4.12$). (□) sample with $T_c \simeq 62$ K at $H=0.25$ T; the solid line is $-|t|^{-2/3}m/T=0.19-0.035\ln|t|^{-4/3}$ and the dashed one $-|t|^{-2/3}m/T=0.0008|t|^{-2/3}$. The arrow marks $t_{abp}\simeq -0.042$ ($\ln|t_{abp}|^{-4/3}\simeq 4.23$).

$$|t|^{-2/3}\frac{m}{T}=-\frac{Q^-c_0^-k_B}{\Phi_0 L_c}\left[\ln\left(\frac{HL_{ab}^2}{\Phi_0}\right)+c_1\right]|t|^{-2/3}=f_0|t|^{-2/3}, \tag{23}$$

and allows to determine L_c, given the amplitude f_0, L_{ab} and c_1. From $\ln|t_{abp}|^{-4/3}\simeq 4.12$ (Fig. 6), $\xi_{ab0}^-\simeq 46.82$ Å [Eq. (21)] and $\ln|t_{abp}|^{-4/3}\simeq 4.46$, $\xi_{ab0}^-\simeq 27.32$ Å we obtain with $\xi_{ab}(t_{abp})=\xi_{ab}^-|t_{abp}|^{-2/3}=L_{ab}$ for the limiting length in the ab plane the estimate

$$L_{ab}\simeq 367\ \text{Å}: \quad T_c\simeq 41.5\ \text{K},$$
$$L_{ab}\simeq 254\ \text{Å}: \quad T_c\simeq 62\ \text{K}, \tag{24}$$

in reasonable agreement with the estimate for their ratio given by Eq. (20). Together with $Q^-c_0^-\simeq -0.7$ [Eq. (9)], $c_1=1.76$ and the rather crude estimates for f_0 (see Fig. 6) Eq. (23) yields

$$L_c\simeq 57\ \text{Å}: \quad T_c\simeq 41.5\ \text{K},$$
$$L_c\simeq 53\ \text{Å}: \quad T_c\simeq 62\ \text{K}, \tag{25}$$

in comparison with the previous estimates $L_{ab}\simeq 392$ Å and $L_c\simeq 52$ Å for $YBa_2Cu_3O_{6.7}$ with $T_c\simeq 59.7$ K, derived from the inhomogeneity induced finite size effect in the temperature dependence of the in-plane penetration depth close to criticality.[30]

Further estimates of the critical amplitudes of the correlation and limiting lengths can be obtained by invoking Eq. (16). According to this we plotted $|t|^{2/3}m/(TH)$ vs t for the sample with $T_c\simeq 41.5$ K and $H=0.2$ T in Fig. 8(a). As t tends to zero the data approaches a minimum around $t=t_{cp}\simeq 0.026$, indicated by the horizontal line and marked by the arrow. This minimum provides an estimate for the critical behavior given by Eq. (16), while the upturn below uncovers again an inhomogeneity induced limiting length along the c axis and in the ab plane. Indeed, when the growth of $\xi_{ab,c}$ are limited by $L_{ab,c}$, $|t|^{2/3}m/(TH)$ tends to zero because the ratio

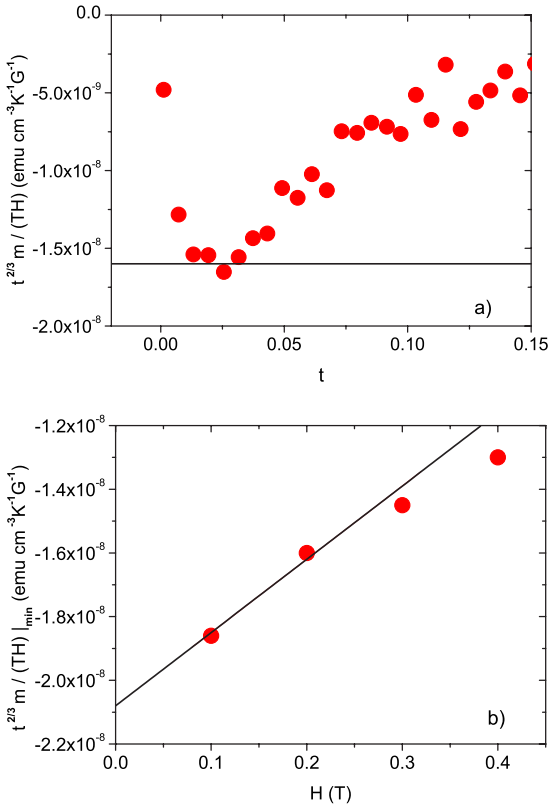

FIG. 8. (Color online) (a) $|t|^{2/3}m/(TH)$ vs t for the sample with $T_c\simeq 41.5$ K and $H=0.2$ T. The horizontal line marks the minimum. (b) $|t|^{2/3}m/(TH)|_{\min}$ vs H for the sample with $T_c\simeq 62$ K and $H=0.25$ T. The line is $|t|^{2/3}m/(TH)|_{\min}=-2.08\times 10^{-8}+2.3\times 10^{-8}H$ with H in T.

ξ_{ab}^2/ξ_c approaches the ratio L_{ab}^2/L_c. A glance to Fig. 8(b) reveals that the minimum exhibits a linear field dependence. Accordingly, the limiting behavior $dG^+/dz=c_0^+z$ [Eq. (8)] is not attained and the lowest magnetic field dependent correction, compatible with the linear dependence, $dG^+/dz=c_0^+z(1+gz)$, must be taken into account. The linear extrapolation yields

$$\frac{Q^+c_0^+k_B(\xi_{ab0}^+)^2}{\Phi_0^2\xi_{c0}^+}=2.08\times 10^{-8}\ (\text{emu cm}^{-3}\ \text{K}^{-1}\ \text{G}^{-1}), \tag{26}$$

and with the universal coefficient $Q^+c_0^+\simeq 0.9$ [Eqs.(9)]

$$(\xi_{ab0}^+)^2/\xi_{c0}^+=\gamma\xi_{ab0}^+\simeq 718\ \text{Å}. \tag{27}$$

Invoking then our estimate for the anisotropy $\gamma\simeq 32.07$ [Eq. (22)] we obtain

$$\xi_{ab0}^+\simeq 22.4\ \text{Å}, \quad \xi_{c0}^+=\xi_{ab0}^+/\gamma\simeq 0.7\ \text{Å}, \tag{28}$$

and with $\xi_{c0}^-\simeq 1.46$ Å [Eq. (19)] for the universal ratio

$$\frac{\xi_{c0}^-}{\xi_{c0}^+}=\frac{\xi_{ab0}^-}{\xi_{ab0}^+}\simeq 2.1, \tag{29}$$

compared to the theoretical prediction $\xi_{c0}^-/\xi_{c0}^+=\xi_{ab0}^-/\xi_{ab0}^+\simeq 2.21$ [Eq. (4)]. Unfortunately, an equivalent analysis of the

TABLE II. Collection of the estimates derived from the magnetization data of Salem-Sugui *et al.* (Refs. 10 and 11) for the underdoped $YBa_2Cu_3O_{7-\delta}$ single crystals. For comparison we included the estimates for nearly optimally doped $YBa_2Cu_3O_{7-\delta}$ (Ref. 17). The bracketed values for ξ^+_{c0} and ξ^+_{ab0} are obtained with Eq. (4). $V^-_{\rm corr}=(\xi^-_{ab0})^2\xi^-_{c0}$ denotes the correlation length volume below T_c. To obtain the critical amplitude of the magnetic in-plane penetration depths λ_{ab0} we used the universal relation (6).

T_c	ξ^-_{c0}	ξ^-_{ab0}	$\gamma=\xi^-_{ab0}/\xi^-_{c0}$	ξ^+_{c0}	$(\xi^+_{ab0})^2/\xi^+_{c0}$	ξ^+_{ab0}	V^-_c	L_{ab}	L_c	$10^{-3}\lambda_{ab0}$	$\lambda_{ab0}/\xi^-_{ab0}$	$10^{-6}\lambda^2_{ab0}T_c$
K	Å	Å		Å	Å	Å	Å^3	Å	Å	Å		Å^2 K
91.7	1.3	10	8				130			0.941	90	81.2
62	1.33	27.32	20.5	(0.60)		(12.36)	993	254	53	1.157	42	83.0
41.5	1.46	46.82	32.07	0.70	718	22.4	3200	367	57	1.482	32	91.1

data for the less underdoped sample with $T_c \simeq 62$ K is not opportune, because the measurements do not extend to comparably low fields.

In Table II we summarized our estimates for the critical properties of underdoped $YBa_2Cu_3O_{7-\delta}$ single crystals derived from the magnetization data of Salem-Sugui *et al.*[10,11] For comparison we included corresponding values for nearly optimally doped $YBa_2Cu_3O_{7-\delta}$.[17] While the critical amplitude of the *c*-axis correlation length $\xi^{\pm}_{c0}$ exhibits a rather weak doping dependence the *ab*-plane counterpart $\xi^{\pm}_{ab0}$ and the anisotropy increase drastically with reduced T_c. As a consequence, the correlation volume $V^-_{\rm corr}=(\xi^-_{ab0})^2\xi^-_c$ increases and the critical amplitude of the specific heat singularity A^- [Eq. (5)] decreases dramatically. This behavior renders it difficult to extract in the underdoped regime critical behavior from specific heat data. Because ξ^-_{c0} does not change much with reduced T_c, the critical amplitude of the in-plane penetration depth λ_{ab0}, resulting from Eq. (6), rises considerably, reflecting the behavior of its zero temperature counterpart $\lambda_{ab}(0)$, where $\lambda_{ab}(0)\simeq 1300$ Å and $\lambda_{ab}(0)\simeq 2250$ Å at $T_c=91.3$ and 60.5 K, respectively.[12] Conversely, although both, the critical amplitudes of the in-plane correlation length ξ^-_{ab0} and penetration depth λ_{ab0} increase with reduced T_c, the ratio $\lambda_{ab0}/\xi^-_{ab0}$, corresponding to the Ginzburg-Landau parameter κ_{ab}, decreases substantially, whereupon $YBa_2Cu_3O_{7-\delta}$ crosses over from an extreme to a weak type-II superconductor. Noting again that the size of the homogeneous domains is not necessarily unique, the onset of the finite size effect probes their respective smallest extent. Accordingly our estimates for L_{ab} and L_c are lower bounds for the extent of the homogenous domains. The estimates for the anisotropy also provide a consistency check for the plots shown in Fig. 6, uncovering the dominant role of 3D-*XY* critical behavior close to T_c. From Eq. (12), Table I and the lines $M/(T_cH)=-3.2\times10^{-11}/H^{1/2}$ and $M/(T_cH)=-2.6\times10^{-11}/H^{1/2}$, indicating the 3D-*XY* critical behavior, we obtain $\gamma(T_c=62\ {\rm K})/\gamma(T_c=41.5\ {\rm K})\simeq 2.6\ 5230/(3.3\ 6300)\cong 0.67$, which is close to 0.64, resulting from the independent estimates listed in Table I. Note that a mean-field analysis of magnetization data, involving the assumption of an upper critical field H_{c2}, yields a growth of ξ^-_{ab0} with reduced T_c as well. From the data of Gao *et al.*[34] we deduce $\xi^-_{ab0}\approx 1200/T_c$ Å with T_c in K. Compared to the 3D-*XY* estimates listed in Table II this approximation underestimates ξ^-_{ab0} in the underdoped and overestimates it in the optimally doped regime. underdoped regime considerably.

In this context it is important to recognize that the listed anisotropies refer to the homogeneous counterparts. However, in the actual inhomogeneous samples these values only apply in an intermediate temperature regime where the growth of the correlation length is not yet limited by the finite size effect. Indeed, considering the sample with $T_c=41.5$ K, below T_c ξ_{ab} levels off around $|t_{abp}|\simeq 0.045$, while ξ_c saturates around $|t_{cp}|\simeq 0.0041$. Accordingly, below $|t_{abp}|$ the anisotropy $\gamma=\xi_{ab}/\xi_c$ decreases from $\gamma=\xi^-_{ab0}/\xi^-_{c0}\simeq 32$ to $\gamma=L_{ab}/L_c\simeq 6.4$ at T_c. This behavior implies that the 2D limit in the underdoped regime is hardly accessible because ξ_{ab} cannot grow beyond L_{ab} and as a result γ does not diverge for fixed ξ_c.

To check the consistency of our analysis further, we invoke Eq. (5) to calculate from the magnetization data the derivative of the universal scaling function in terms of

$$Q^{\pm}\frac{dG^{\pm}}{dz}=-\frac{m}{T}\frac{\Phi_0}{k_B}\xi^{\pm}_{c0}|t|^{-2/3},\quad z=[H(\xi^{\pm}_{ab0})^2/\Phi_0]|t|^{-4/3}, \tag{30}$$

and the respective estimates for the critical amplitudes of the correlation lengths (Table II). In Fig. 9(a), showing $-Q^-dG/dz$ vs $\ln(z)$ below T_c, we observe from $\ln(z)\simeq -2.75$ down to -4.25 consistency with the leading $z\to 0$ behavior $Q^-dG/dz=Q^-c^-_0[\ln(z)+c_1]$, where $Q^-c^-_0=-0.7$ [Eq. (9)] and c_1 was chosen as

$$c_1=1.76. \tag{31}$$

This estimate fixes the so far unknown universal coefficient c_1. The systematic deviations, setting in around $\ln(z)\simeq -2.75(z\simeq 0.065)$, uncover the onset of the inhomogeneity induced finite size effect, limiting the growth of ξ_{ab}. Indeed, this value corresponds to $z=HL^2_{ab}/\Phi_0$ with $H=0.1$ T and $L_{ab}=367$ Å (Table II). On the other hand, the upturn setting in around $\ln(z)\simeq -4.2(z\simeq 0.0136)$ signals the escape from the scaling regime where the $\ln(z)$ behavior applies. Indeed, in the present case H is fixed and the reduction of $z=[H(\xi^+_{ab0})^2/\Phi_0]|t|^{-4/3}$ unavoidably implies an increasing reduced temperature t and with that a run away from criticality. Thus, for fixed magnetic field the window where the universal scaling function can be observed is limited from below by the run away from criticality and from above by the finite size effect in ξ_{ab}. The inset in Fig. 9 shows $Q^+d^2G^+/dz^2=-d[m\xi^-_{c0}|t|^{-2/3}\Phi_0/(k_BT)]/dz$ vs $z=[H(\xi^+_{ab0})^2/\Phi_0]|t|^{-4/3}$. According to Eq. (9) it approaches in a homogenous system in

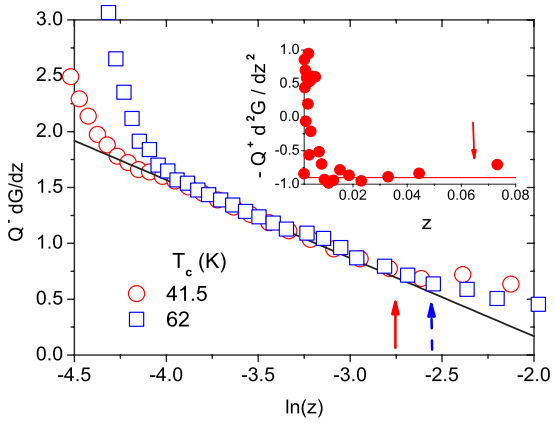

FIG. 9. (Color online) $Q^-dG^-/dz=-(m\Phi_0/Tk_B)\xi_{c0}^-|t|^{-2/3}$ vs $\ln(z)$ for the sample with $T_c=41.5$ K at $H=0.1$ T, $\xi_{ab0}^-=46.82$ Å and $\xi_{c0}^-=1.46$ Å (○) and the sample with $T_c=62$ K at $H=0.25$ T, $\xi_{ab0}^-=27.32$ Å and $\xi_{c0}^-=1.33$ Å (□); the solid line is $Q^-dG^-/dz=Q^-c_0^-[\ln(z)+c_1]$ with $z=[H(\xi_{ab0}^-)^2/\Phi_0]|t|^{-4/3}$, $Q^-c_0^-=-0.7$ [Eq. (9)], and $c_1=1.76$ [Eq. (31)]. The arrows mark the onset of the finite size effect in ξ_{ab} at $\ln(z)=HL_{ab}^2/\Phi_0$, namely, $\ln(z)=-2.73$ ($T_c=41.5$ K) and $\ln(z)=-2.55$ ($T_c=62$ K). The inset shows $Q^+d^2G^+/dz^2=-d[m(\Phi_0/Tk_B)\xi_{c0}^-|t|^{-2/3}]/dz$ vs $z=[H(\xi_{ab0}^+)^2/\Phi_0]|t|^{-4/3}$ with $T_c=41.5$ K for $\xi_{ab0}^+=22.4$ Å and $\xi_{c0}^+=0.7$ Å; the solid line is $Q^+d^2G^+/dz^2=Q^+c_0^+$ with $Q^+c_0^+\simeq 0.9$ [Eq. (9)]. The arrow marks $z=HL_{ab}^2/\Phi_0\simeq 0.065$, the onset of the finite size effect in ξ_{ab}.

the limit $z\to 0$ the universal value $Q^+d^2G^+/dz^2=Q^+c_0^+\simeq 0.9$. Even though the available data are rather sparse we observe in the interval $0.01\lesssim z\lesssim 0.04$ consistency with this limiting behavior, indicated by the horizontal line. Unfortunately, the available data do not allow to locate the onset of the finite size effect in ξ_{ab}, seen below T_c around $\ln(z)=\ln(HL_{ab}^2/\Phi_0)\simeq\ln(0.065)\simeq -2.73$. The upturn setting in around $z=0.01$ signals the runaway from criticality.

Next we turn to magnetization data of Babíc *et al.*,[5] taken at fixed temperatures below T_c as a function of the magnetic field applied along the c axis. Here we analyze the data of the $YBa_2Cu_3O_{7-\delta}$ single crystal with $T_c\simeq 93.5$ K. In Fig. 10 we show M vs $\ln(H)$. In a limited interval we observe linear behavior so that the scaling form (13) rewritten in the form

$$M=-\frac{VQ^-c_0^-k_BT}{\Phi_0\xi_c}\left[\ln(H)+\ln\left(\frac{\xi_{ab}^2}{\Phi_0}\right)+c_1\right]=d+e\ln(H), \tag{32}$$

applies. The solid lines are this scaling form with the parameters d and e listed in Table III.

Given the volume of the sample, the universal amplitudes $Q^-c_0^-\simeq -0.9$ [Eq. (9)] and c_1 [Eq. (31)] the listed correlation lengths are then readily calculated. Together with $\xi_{ab,c}=\xi_{ab0,c0}^-|t|^{-2/3}$ we obtain for the critical amplitudes the estimates

$$\xi_{ab0}^-\simeq 7\ \text{Å},\quad \xi_{c0}^-\simeq 1.4\ \text{Å}, \tag{33}$$

in comparison with $\xi_{ab0}^-\simeq 10.4$ Å and $\xi_{c0}^-\simeq 1.3$ Å for the sample with $T_c=91.7$ K (Table II).

To check the consistency with the scaling form ([?]) fur-

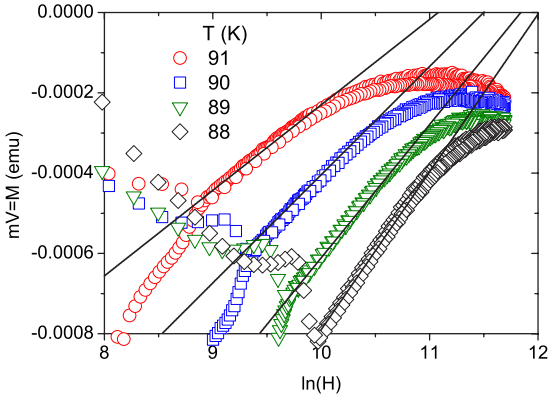

FIG. 10. (Color online) M vs $\ln(H)$ for various temperatures derived from the data of Babíc *et al.* (Ref. 5) for a $YBa_2Cu_3O_{7-\delta}$ single crystal with $T_c\simeq 93.5$ K and the magnetic field applied along the c axis. The solid lines are Eq. (32) with the parameters listed in Table III.

ther, we calculated $m\Phi_0\xi_c/(k_BT)=-Q^-dG^-/dz$ vs z for $T=91$ and 90 K as shown in Fig. 11 with the parameters listed in Table III. The comparison with the leading $z\to 0$ behavior $-Q^-dG^-/dz=-Q^-c_0^-[\ln(z)+c_1]$ reveals that this regime is attained, but limited by irreversibility in the limit $z\to 0$ and the crossover to the large z limit $-Q^-dG^-/dz=-qz^{1/2}$ with $q\simeq 0.5$ [Eq. (9)]. This limitation is also apparent in Fig. 10 on the low and high field side. Indeed, because the data do not extend close to T_c, the correlation lengths are comparatively small and their growths is not yet limited by the extent of the homogenous domains.

Although the analyzed magnetization data is afflicted with uncertainties arising from the subtraction of the normal state paramagnetism and the Curie term due to paramagnetic impurities or defects, we observed remarkable consistency with 3D-XY critical behavior for both, nearly optimally doped and underdoped samples. In contrast to previous work[4,5] we did not establish the consistency with the 3D-XY scaling plots only, but estimated, given the critical exponent of the correlation lengths $\nu\simeq 2/3$, the critical amplitudes of the correlation length, the universal ratios, etc., of the associated fictitious homogeneous system as well. Indeed, the universality

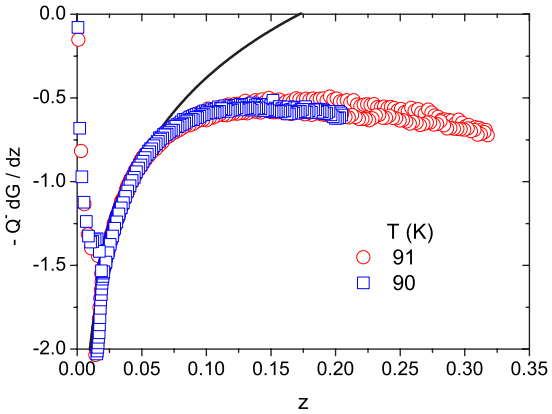

FIG. 11. (Color online) $m\Phi_0\xi_c/(k_BT)=-Q^-dG^-/dz$ vs z for $T=91$ and 90 K. The solid line is $-Q^-dG^-/dz=-Q^-c_0^-[\ln(z)+c_1]$ with $Q^-c_0^-=-0.7$ [Eq. (9)], $c_1=1.76$ [Eq. (31)].

TABLE III. Parameters entering Eq. (32), yielding the straight lines in Fig. 11 and with $Q^{-}c_0^{-}=-0.7$ [Eq. (9)], $c_1=1.76$ [Eq. (31)], and $V=8.2\times10^{-4}$ cm^{-3} (Ref. 5) the estimates for the correlation lengths ξ_{ab} and ξ_c.

T (K)	d (emu)	e (emu)	ξ_{ab} (Å)	ξ_c (Å)
91	-2.36×10^{-3}	2.13×10^{-4}	74.1	16.3
90	-3.10×10^{-3}	2.70×10^{-4}	59.5	12.8
89	-3.93×10^{-3}	3.32×10^{-4}	50.7	10.3
88	-4.72×10^{-3}	3.93×10^{-4}	46.5	8.8

class to which a given experimental system belongs is not only characterized by its critical exponents but also by various critical point amplitude ratios and universal coefficients. This has been achieved by invoking the limiting behavior of the universal scaling function dG/dz, allowing via Eqs. (13)–(16) to explore the growth of the in-plane and c-axis correlation lengths as T_c is approached from below or above. We have seen that this growth is limited due to inhomogeneities and that this limitation appears to be equivalent to a finite size effect, whereupon the correlation lengths cannot grow beyond the extent of the homogenous domains. Clearly, such an analysis does not discriminate between intrinsic or extrinsic inhomogeneities, but it provides lower bounds for the extent of the homogenous domains seen by the relevant fluctuations. Even though since the discovery of superconductivity in the cuprates by Bednorz and Müller[35] a tremendous amount of work has been devoted to their characterization, the issue of inhomogeneities and their characterization is still a controversial issue. There is neutron spectroscopic evidence for nanoscale cluster formation and percolative superconductivity in various cuprates.[36,37] Nanoscale spatial variations in the electronic characteristics have been observed in underdoped $Bi_2Sr_2CaCu_2O_{8+\delta}$ with scanning tunneling microscopy.[38–41] They reveal a spatial segregation of the electronic structure into 3-nm-diameter superconducting domains in an electronically distinct background. Furthermore, the investigations of Gauzzi *et al.*[42] on $YBa_2Cu_3O_{6.9}$ films with reduced long-range structural order clearly reveals that the size of the homogeneous domains strongly depends on the growth conditions. In any case we have shown that the analysis of reversible magnetization data taken near criticality does not uncover the critical properties of the associated fictitious homogenous and infinite system only, but provides lower bounds for the extent of the homogeneous domains as well. Last but not least, having established the consistency with 3D-*XY* universality there are universal relations such as Eqs. (4)–(6) and (10). They imply that the effect of pressure and isotope exchange on the respective properties are not independent.

The author is grateful to S. Salem-Sugui, Jr. and J. R. Cooper for providing the magnetization data.

*Electronic address: toni.schneider@physik.unizh.ch

[1] T. Schneider and J. M. Singer, *Phase Transition Approach To High Temperature Superconductivity* (Imperial College Press, London, 2000).
[2] T. Schneider, in *The Physics of Superconductors*, edited by K. Bennemann and J. B. Ketterson (Springer, Berlin, 2004), p. 111.
[3] T. Schneider, Phys. Rev. B **67**, 134514 (2003).
[4] M. A. Hubbard, M. B. Salamon, and B. W. Veal, Physica C **259**, 309 (1996).
[5] D. Babíc, J. R. Cooper, J. W. Hodby, and Chen Changkang, Phys. Rev. B **60**, 698 (1999).
[6] J. Hofer, T. Schneider, J. M. Singer, M. Willemin, H. Keller, T. Sasagawa, K. Kishio, K. Conder, and J. Karpinski, Phys. Rev. B **62**, 631 (2000).
[7] T. Schneider, Physica B **326**, 289 (2003).
[8] T. Schneider, R. Khasanov, K. Conder, E. Pomjakushina, R. Bruetsch, and H. Keller, J. Phys.: Condens. Matter **16**, L 437 (2004).
[9] Y. Ando and K. Segawa, Phys. Rev. Lett. **88**, 167005 (2002).
[10] S. Salem-Sugui Jr., A. D. Alvarenga, K. C. Goretta, V. N. Vieira, B. Veal, and A. P. Paulikas, J. Low Temp. Phys. **141**, 83 (2005).
[11] S. Salem-Sugui Jr., A. D. Alvarenga, B. Veal, and A. P. Paulikas, J. Low. Temp. Phys. (to be published).
[12] P. Zimmermann *et al.*, Phys. Rev. B **52**, 541 (1995).
[13] B. Janossy, D. Prost, S. Pekker, and L. Fruchter, Physica C **181**, 51 (1991).
[14] D. S. Fisher, M. P. A. Fisher, and D. A. Huse, Phys. Rev. B **43**, 130 (1991).
[15] T. Schneider and D. Ariosa, Z. Phys. B: Condens. Matter **89**, 267 (1992).
[16] T. Schneider and H. Keller, Int. J. Mod. Phys. B **8**, 487 (1993).
[17] T. Schneider, J. Hofer, M. Willemin, J. M. Singer, and H. Keller, Eur. Phys. J. B **3**, 413 (1998).
[18] J. Hofer, T. Schneider, J. M. Singer, M. Willemin, H. Keller, C. Rossel, and J. Karpinski, Phys. Rev. B **60**, 1332 (1999).
[19] A. Peliasetto and E. Vicari, Phys. Rep. **368**, 549 (2002).
[20] R. E. Prange, Phys. Rev. B **1**, 2349 (1970).
[21] N. Overend, M. A. Howson, and I. D. Lawrie, Phys. Rev. Lett. **72**, 3238 (1994).
[22] S. Kamal, D. A. Bonn, N. Goldenfeld, P. J. Hirschfeld, R. Liang, and W. N. Hardy, Phys. Rev. Lett. **73**, 1845 (1994).
[23] Y. Jaccard, T. Schneider, J.-P. Looquet, E. J. Williams, P. Martinoli, and Ø. Fischer, Europhys. Lett. **34**, 281 (1996).
[24] S. Kamal, R. Liang, A. Hosseini, D. A. Bonn, and W. N. Hardy, Phys. Rev. B **58**, R8933 (1998).
[25] V. Pasler, P. Schweiss, Ch. Meingast, B. Obst, H. Wühl, A. I. Rykov, and S. Tajima, Phys. Rev. Lett. **81**, 1094 (1998).
[26] M. Roulin, A. Junod, and E. Walker, Physica C **296**, 137 (1998).
[27] A. B. Harris, J. Phys. C **7**, 1671 (1974).
[28] *Finite-Size Scaling*, edited by J. L. Cardy (North-Holland, Amsterdam, 1988).
[29] V. Privman, *Finite Size Scaling and Numerical Simulations of Statistical System* (World Scientific, Singapore, 1990).
[30] T. Schneider and D. Di Castro, Phys. Rev. B **69**, 024502 (2004).

[31] L. Li *et al.*, Europhys. Lett. **72**, 451 (2005).
[32] S. Salem-Sugui, Jr., A. D. Alvarenga, V. N. Vieira, and O. F. Schilling, Phys. Rev. B **73**, 012509 (2006).
[33] D. R. Harshman and A. P. Mills, Phys. Rev. B **45**, 10684 (1992).
[34] Hong Gao, C. Ren, L. Shan, Y. Wang, Y. Zhang, S. Zhao, X. Yao, and H. H. Wen, Phys. Rev. B **74**, 020505(R) (2006).
[35] G. Bednorz and K. A. Müller, Z. Phys. B: Condens. Matter **64**, 189 (1986).
[36] J. Mesot, P. Allenspach, U. Staub, A. Furrer, and H. Mutka, Phys. Rev. Lett. **70**, 865 (1993).
[37] A. Furrer *et al.*, Physica C **235-240**, 261 (1994).
[38] J. X. Liu, J. C. Wan, A. M. Goldman, Y. C. Chang, and P. Z. Jiang, Phys. Rev. Lett. **67**, 2195 (1991).
[39] A. Chang, Z. Y. Rong, Y. M. Ivanchenko, F. Lu, and E. L. Wolf, Phys. Rev. B **46**, 5692 (1992).
[40] T. Cren, D. Roditchev, W. Sacks, J. Klein, J.-B. Moussy, C. Deville-Cavellin, and M. Laguës, Phys. Rev. Lett. **84**, 147 (2000).
[41] K. M. Lang, V. Madhavan, J. E. Hoffman, E. W. Hudson, H. Eisaki, S. Uchida, and J. C. Davis, Nature (London) **415**, 413 (2002).
[42] A. Gauzzi *et al.*, Europhys. Lett. **51**, 667 (2000).